An Ultra-Broadband Fiber Grating Coupler with Focusing Curved Subwavelength Structures

Qiuhang Zhong[1,*], Wei Shi[1,2], Yun Wang[3], Lukas Chrostowski[3], and David V. Plant[1]
[1]*Department of Electrical and Computer Engineering, McGill University, Montreal, QC, H3A 2A7, Canada*
[2]*Department of Electrical and Computer Engineering, Université Laval, Québec, QC, GIK 7P4, Canada*
[3]*Department of Electrical and Computer Engineering, University of British Columbia, Vancouver, BC, V6T 1Z4, Canada*
[*]*qiuhang.zhong@mail.mcgill.ca*

Abstract: We demonstrate the first fiber grating coupler with focusing curved subwavelength structures. An ultra-wide 1-dB bandwidth of over 100 nm with -6.7 dB coupling efficiency at 1550 nm has been experimentally achieved.
OCIS codes: (050.2770) Gratings; (050.6624) Subwavelength structures.

1. Introduction

CMOS-compatible silicon photonics is promising for future chip-level optical interconnects [1]. Fiber-to-chip coupling is essential for silicon photonic integrated circuits (Si-PICs) as the optical interface. Edge coupling and surface coupling are two major solutions for the optical interface of Si-PICs. Surface coupling, utilizing diffraction fiber grating couplers (FGCs) to collect light, has advantages over edge coupling in terms of simplicity of fabrication, flexibility of interface positions, capability of wafer-scale test, ease of alignment and potentially low cost of packaging [2]. However, compared to edge coupling, FGCs have relatively narrow bandwidths, which are intrinsically limited by waveguide dispersion [3]. For many optical interconnects applications such as wavelength-division multiplexing (WDM) systems, a broadband optical interface is highly desired. While most previous works have focused on increasing the efficiency of FGCs [4-6], only a few attempts to improve the bandwidth have been reported so far [3,7,8].

In this paper, we present the first design of a focusing curved subwavelength FGC with ultra-wide bandwidth and relatively high efficiency for Si-PIC optical interface. The improvement of bandwidth relies on suppressing the waveguide dispersion by applying subwavelength structures to reduce the average grating effective refractive index. Using the finite-difference time-domain (FDTD) method, we optimized the grating parameters based on the trade-off between bandwidth and efficiency. We designed focusing geometric gratings with curved subwavelength structures, which is much more compact than conventional straight-line grating designs [9]. The FGC devices were fabricated by electron-beam lithography (EBL) in a single-step full-etching, which is more cost-efficient than two-step process including partial- and full-etching. The experimental results are in good agreement with the simulation, and a 1-dB bandwidth of over 100 nm with -6.7 dB coupling efficiency at 1550 nm is experimentally achieved. To the best of our knowledge, this work is the first demonstration of focusing curved subwavelength FGCs. The achieved 1-dB bandwidth is the largest of FGCs, and the device footprint (40 μm × 40 μm) is the smallest of subwavelength FGCs reported to date.

2. Principle and simulation

According to [8] and [10], the bandwidth of a FGC can be generally approximated by:

$$BW = \eta \frac{n_c \cos\theta}{\left| \frac{n_{eff}(\lambda_o) - n_c \sin\theta}{\lambda_o} - \frac{dn_{eff}(\lambda)}{d\lambda} \right|}, \quad (1)$$

where η is a fiber-related coefficient, n_c is the cladding refractive index, θ is the coupling angle, n_{eff} is the grating effective refractive index, and λ_o is the center coupling wavelength. The dispersion term $dn_{eff}(\lambda)/d\lambda$ in Eq. (1) is negative for silicon waveguide. At a fixed wavelength, the dispersion decreases (in terms of absolute value) with the decrease of effective refractive index of the grating, as the light confinement is looser. According to Eq. (1), the decrease of dispersion (approaching zero from negative values) can lead to a larger bandwidth. Hence, for a fixed material system, coupling angle and wavelength, the most feasible approach to increase the bandwidth of a FGC is to reduce the grating effective refractive index.

The grating effective refractive index can be dramatically reduced by applying subwavelength structures [3,8]. According to effective medium theory [3], a periodic subwavelength region can be treated as a uniform material

with an effective index equal to the weighted average of the material indices of silicon and the cladding. Then the subwavelength structures can be designed as periodically interleaved regions with high and low indices, as shown in Fig. 1(a). Reducing the grating effective refractive index can both improve the bandwidth and affect the coupling efficiency, because the index contrast between cladding and grating is also reduced [8]. In order to achieve a good compromise between bandwidth and efficiency, we optimized the grating design by tuning critical parameters such as grating period, filling factor, and effective indices. We chose the product of 1-dB bandwidth and coupling efficiency at 1550 nm as the figure of merit for optimization. The simulation and optimization were conducted using 2-D FDTD for transverse-electric (TE) polarized light with an incident angle of 20°. The best result was obtained with a grating period of 1.16 μm, a filling factor of 0.6, and effective indices of 2.79 and 1.71 at 1550 nm for the high and low index regions, respectively. Considering the subwavelength condition [11] and the feasible minimum feature size of EBL, we chose a subwavelength grating period of 0.3 μm (with a direction perpendicular to the FGC's gratings), subwavelength filling factors of 0.67 and 0.13 for the high and low index regions, respectively. All these grating parameters are illustrated in Fig. 1(b).

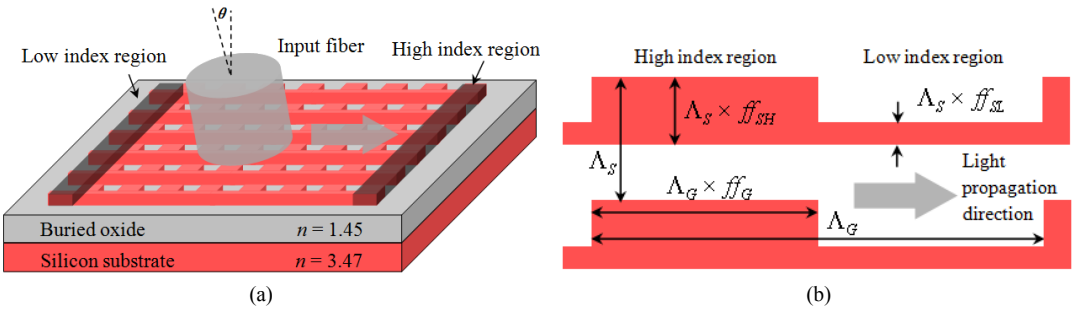

Fig. 1. (a) 3-D schematic illustration of the periodic subwavelength structures with interleaved high and low index regions. (b) Top-view schematic of a cycled region of the periodic subwavelength structures. Λ_G and ff_G are the grating period and filling factor, Λ_S is the subwavelength grating period, ff_{SH} and ff_{SL} are the subwavelength filling factors of the high and low index region, respectively.

3. Experiment and results

The focusing curved subwavelength FGCs were fabricated on silicon-on-insulator (220-nm silicon on 3-μm buried oxide) with oxide cladding using EBL. For comparison, gratings with straight-line subwavelength structures were also fabricated. Multiple FGCs with parameter variations around the optimal values were fabricated. The scanning electron microscopy (SEM) images of the two kinds of gratings are shown in Fig. 2(a) and (b), with oxide cladding removed. The focusing curved subwavelength FGC shown in Fig. 2(a) has subwavelength filling factors of 0.5 and 0, and the straight-line design shown in Fig. 2(b) has parameters close to the optimal values. The inset of Fig. 2(b) gives a zoomed view of the interleaved subwavelength gratings with a minimum feature size of ~ 40 nm. The total footprint of the straight-line design is 520 μm × 20 μm, including a 500-μm linear taper used to adiabatically convert the optical mode from the 20-μm-wide grating to the 500-nm-wide waveguide with low loss. In the curved design, grating lines are a series of con-focal ellipses with the focus located at the starting point of a short taper. By choosing curving parameters according to the phase match condition derived in [9], light can be directly focused from the grating to the waveguide, obviating the long adiabatic mode conversion. Thereby the focusing curved FGC has a much smaller footprint (40 μm × 40 μm) and yields a higher degree of integration than the straight-line FGC.

The devices under test consist of a pair of input and output subwavelength FGCs with 127 μm pitch, connected by a short strip waveguide with neglectable loss. A fiber array ribbon is used to test these FGCs on the setup described in [12]. The measured transmission spectra of focusing curved and straight-line subwavelength FGCs are shown as red and blue curves in Fig. 2(c), respectively. Across the entire measured spectral range (1490-1610 nm, limited by the tunable laser), the transmission spectra are very flat, indicating ultra-wide bandwidths. The 1-dB bandwidths of the two FGCs are both over 100 nm. The coupling efficiencies at 1550 nm are -6.7 dB and -7.8 dB for the focusing curved and straight-line designs, respectively. These results show that the focusing curved design introduces no performance penalty while dramatically reducing the footprint compared to the straight-line design. For comparison, the simulated transmission spectrum of the subwavelength FGC with optimized parameters is also plotted as black curve in Fig. 2(c). The calculated 1-dB bandwidth reaches 112 nm with an efficiency of -2.9 dB at 1550 nm. The trend of the measured spectra agrees well with the simulation, while the efficiency is much lower. This can be explained as follows. The fiber array ribbon has a cleaving angle of ~ 20°. According to Snell's Law, when the fiber end is parallel to the chip, the light incident angle is ~ 30° in the air. Hence, to reach the optimized coupling angle (20°), the fiber need to be rotated, inducing an air gap between the fiber end and the chip. Extra

distance is also kept to ensure the fiber would not scratch the chip. When light propagates in this air gap, the optical mode profile becomes larger, which brings extra loss [13].

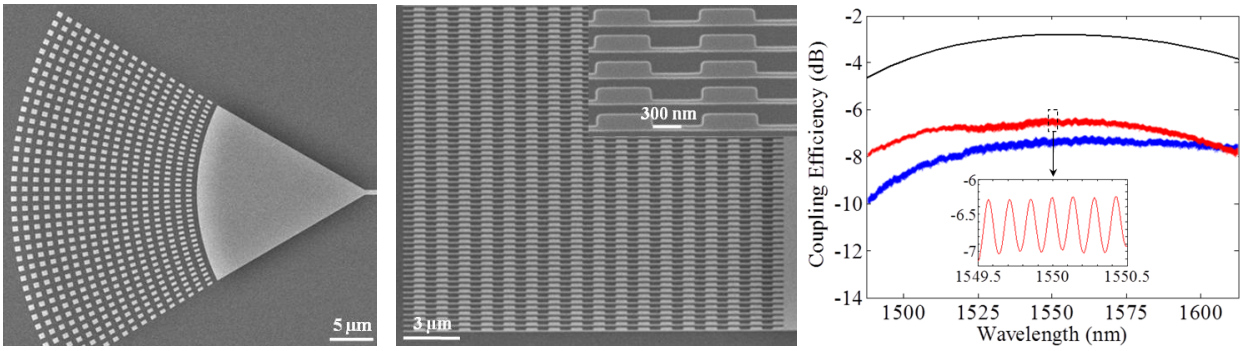

(a) (b) (c)

Fig. 2. SEM images of fabricated subwavelength FGCs: (a) focusing curved (ff_{SL} = 0) and (b) straight-line (ff_{SL} = 0.13) designs. (c) Calculated (black) and measured (red: focusing curved design, blue: straight-line design) coupling efficiency versus wavelength of the subwavelength FGCs. Inset of (b) shows the detail of the interleaved subwavelength gratings. Inset of (c) shows the measured Fabry-Perot ripples near 1550 nm.

It should be noted that in order to achieve the engineered refractive indices, only one step of full-etch is conducted in the fabrication process. This saves the additional partial-etch required by regular high efficiency FGCs, minimizing the fabrication complexity and cost. However, full-etched FGCs tend to have larger back reflection and thus lower efficiency than partial-etched ones. As shown in the inset of Fig. 2(c), there exist small ripples in the measured spectra. These ripples are originated from the Fabry-Perot interference induced by the Fresnel reflections at the interfaces between cladding and silicon. Compared with regular full-etched FGCs, the extinction ratio of the ripples in the subwavelength design is relatively low (~ 0.7 dB versus 4 dB) [12]. This can be attributed to the implementation of subwavelength structures, which mitigate the index contrast between the cladding and silicon. Works are still in progress to improve the efficiency while maintaining the wide bandwidth. The back reflection can be reduced by adopting subwavelength gradient-index (GRIN) anti-reflective (AR) structures [14]. Apodizing the grating in the light propagation direction is another promising approach to further increase the efficiency [5].

4. Conclusion

In summary, we have presented the first demonstration of a focusing curved subwavelength FGC for Si-PIC optical interface. By applying the optimized subwavelength structures, we have experimentally achieved a 1-dB bandwidth of over 100 nm (largest reported in FGCs to date) with -6.7 dB coupling efficiency at 1550 nm. By utilizing the focusing curved grating design, we have minimized the footprint of the FGC to be only 40 μm × 40 μm (the most compact of subwavelength FGCs realized to date).

Acknowledgement

The authors thank CMC Microsystems for supporting this work, Lumerical Solutions and Mentor Graphics for the software and design support. The devices were fabricated by R. Bojko at the University of Washington Microfabrication/Nanotechnology User Facility, a member of the NSF National Nanotechnology Infrastructure Network. This work is supported by Natural Sciences and Engineering Research Council of Canada (NSERC), particularly under the Silicon Electronic-Photonic Integrated Circuits (Si-EPIC) CREATE program.

References

[1] M. Asghari, et al, Nat. Photon. **5**(5), 268-270 (2011).
[2] A. Mekis,et al, JSTQE **17**(3), 597-608 (2011).
[3] X. Chen, et al, OL **37**(17), 3483-3485 (2012).
[4] F. V. Laere, et al, JLT **25**(1), 151-156 (2007).
[5] X. Chen, et al, PTL **22**(15), 1156-1158 (2010).
[6] D. Vermeulen, et al, OE **18**(17), 18278-18282 (2010).
[7] Z. Xiao, et al, OL **37**(4), 530-532 (2012).
[8] X. Xu, et al, OL **38**(18), 3588-3591 (2013).
[9] F. V. Laere, et al, PTL **19**(23), 1919-1921 (2007).
[10] Z. Xiao, et al, OE **21**(5), 5688-5700 (2013).
[11] P. J. Bock, et al, OE **18**(15), 16146-16155 (2010).
[12] Y. Wang, et al, in Proc. SPIE Photonics North (2013).
[13] Y. Wang, Master thesis, University of British Columbia (2013).
[14] J. H. Schmid, et al, OL **32**(13), 1794-1796 (2007).